Contents lists available at ScienceDirect

Systems & Control Letters

Improved residual mode separation for finite-dimensional control of PDEs: Application to the Euler–Bernoulli beam

Anton Selivanov [a] [iD],*, Emilia Fridman [b]

[a] *School of Electrical and Electronic Engineering, The University of Sheffield, Sheffield, UK*
[b] *School of Electrical Engineering, Tel Aviv University, Tel Aviv, Israel*

ARTICLE INFO

ABSTRACT

We consider a simply-supported Euler–Bernoulli beam with viscous and Kelvin–Voigt damping. Our objective is to attenuate the effect of an unknown distributed disturbance using one piezoelectric actuator. We show how to design a state-feedback controller based on a finite number of dominating modes that guarantees that the L^2 gain is not greater than a given value. If the remaining (infinitely many) modes are simply ignored, the calculated L^2 gain is wrong. This happens because of the spillover phenomenon that occurs when the effect of the control on truncated modes is not accounted for in the feedback design. We propose a simple modification of the H_∞ cost that prevents spillover. The key idea is to treat the control as a disturbance in the truncated modes and find the corresponding L^2 gains using the bounded real lemma. These L^2 gains are added to the control weight in the H_∞ cost for the dominating modes, which prevents spillover. A numerical simulation of an aluminum beam with realistic parameters demonstrates the effectiveness of the proposed method. The presented approach is applicable to other types of PDEs, such as the heat, wave, and Kuramoto–Sivashinsky equations, as well as their semilinear versions. The proposed method gives a Lyapunov functional that can also be used for guaranteed cost control, regional stability analysis, and input-to-state stability.

1. Introduction

The H_∞ control theory enables the design of controllers robust to modeling errors, measurement noise, and unknown disturbances [1, 2]. Its extension to *infinite*-dimensional systems is challenging, especially if the controller is required to be *finite*-dimensional. In particular, the direct extension of the *frequency-domain* approach results in infinite-dimensional controllers [3,4], which are then approximated by finite-dimensional ones [5–7]. The approximation leads to performance degradation known as spillover, which can be characterized via the H_∞ norm of the approximation error [8]. The frequency-domain approach, which is very natural for H_∞ control, may be difficult to use in the infinite-dimensional case since the transcendental transfer function of an infinite-dimensional plant may be hard to find [9], its inner-outer factorization required for the design is not straightforward [4], and the MIMO case requires restrictive assumptions [3]. Furthermore, the frequency-domain approach is not applicable to guaranteed cost control, regional stability analysis, systems with time-varying delays, and nonlinear systems.

The *time-domain* approach avoids these restrictions. Its direct extension to infinite-dimensional systems leads to an operator Riccati equation, which also results in an infinite-dimensional controller [10,

11]. To obtain a finite-dimensional controller, one can perform modal decomposition [12,13] and design a controller for a finite number of dominating modes [14–16]. Similarly to the frequency-domain design, this leads to spillover: neglected modes deteriorate the overall system performance [17,18]. Nevertheless, *stability* under spillover can be guaranteed using residual filters [19–21] or spectral properties of linear operators representing the dynamics [22,23].

The time-domain *performance* analysis under spillover is more challenging than the stability analysis and requires careful treatment of the neglected modes. Such treatment has been provided for parabolic PDEs in [24–27] with subsequent extensions to input/output delays [28–30], semilinear systems [31,32], as well as the Kuramoto–Sivashinsky [33], wave [34], and Euler–Bernoulli [35] equations.

This paper proposes a new way of dealing with spillover in the time domain. Namely, we treat the control input as a disturbance in the residue modes and explicitly solve the algebraic Riccati equation for each neglected mode to find the input-to-state L^2 gains. These gains are added to the control weight in the cost used to design a state-feedback controller that guarantees that the L^2 gain is not greater than a given value. This idea leads to a simple yet efficient way of designing a finite-dimensional controller that avoids spillover. The analysis is

---

based on the cost decomposition presented in Section 3.3. We develop this idea to attenuate disturbances in the Euler–Bernoulli beam with piezoelectric actuators, which is of great importance for aerospace, civil, and mechanical engineering. Using a numerical example of an aluminum beam, we demonstrate a drastic improvement compared to our previous results in [35]. Namely, spillover is avoided using just 8 modes instead of 32, and we prove that the L^2 gain can only decrease when more modes are considered.

The frequency-domain approach to the H_∞ control of beams was developed in [36–38], the controllability problem under piezoelectric actuators was studied in [39–41], and experimental results (without spillover analysis) were reported in [42,43]. Here, we develop the time-domain method, which, differently from the frequency-domain approach, can be extended to guaranteed cost control and regional stability analysis. Furthermore, the proposed idea can significantly improve the finite-dimensional controller design for other types of PDEs, including the heat, wave, and Kuramoto–Sivashinky equations. It also admits an extension to semilinear PDEs in a manner similar to [31,32].

Notations: $|\cdot|$ is the Euclidean norm, $\|\cdot\|$ is the L^2 norm, $\langle\cdot,\cdot\rangle$ is the scalar product in L^2, $H^p(0,\pi)$ with $p \in \mathbb{N}$ are the Sobolev spaces, $H^{-p}(0,\pi)$ are their dual spaces, $H^1_{loc}(0,\infty)$ are the functions that belong to $H^1(K)$ for any compact $K \subset (0,\infty)$, $\mathrm{diag}\{\omega_1,\ldots,\omega_N\}$ is the diagonal matrix with diagonal elements ω_n, $n = 1,\ldots,N$. For a matrix P, the notation $P < 0$ implies that P is square, symmetric, and negative-definite. Partial derivatives are denoted by indices, e.g., $z_t = \partial z/\partial t$.

1.1. Preliminaries: H_∞ control of finite-dimensional systems

Consider the LTI system

$$
\begin{aligned}
\dot{x}(t) &= Ax(t) + Bu(t) + Ev(t), \qquad x(0) = 0, \\
y(t) &= Cx(t) + Du(t)
\end{aligned}
\tag{1}
$$

with state $x \in \mathbb{R}^n$, control input $u \in \mathbb{R}^m$, disturbance $v \in \mathbb{R}^k$, controlled output $y \in \mathbb{R}^l$, and constant matrices A, B, C, D, and E. We say that $u = -Kx$ with $K \in \mathbb{R}^{m\times n}$ guarantees that the L^2 gain from v to y is not greater than $\gamma > 0$ if the solutions of the closed-loop system satisfy

$$
\int_0^\infty \left[|y(t)|^2 - \gamma^2 |v(t)|^2 \right] dt \leq 0, \quad \forall v \in L^2([0,\infty), \mathbb{R}^k).
\tag{2}
$$

That is, the H_∞ norm of the closed-loop transfer function from v to y is not greater than γ. The proofs of the following results are given, e.g., in [2].

Proposition 1. *Consider* (1) *such that* $D^\top C = 0$ *and* $R = D^\top D > 0$. *Given* $\gamma > 0$, *let* $0 < P \in \mathbb{R}^{n\times n}$ *satisfy*

$$
PA + A^\top P - P(BR^{-1}B^\top - \gamma^{-2}EE^\top)P + C^\top C = 0.
\tag{3}
$$

Then $u(t) = -R^{-1}B^\top Px(t)$ *guarantees* (2).

Remark 1 (*Solution Existence*)**.** If (A, B) is stabilizable, (A, C) is detectable, and γ is large enough, then (3) has a solution. For this solution, the closed-loop matrix $A - BR^{-1}B^\top P$ is stable.

Corollary 1 (*Bounded Real Lemma*)**.** *Consider* (1) *with* $B = 0$ *and* $D = 0$ *(i.e., without control). Given* $\gamma > 0$, *let* $0 < P \in \mathbb{R}^{n\times n}$ *satisfy*

$$
PA + A^\top P + \gamma^{-2}PEE^\top P + C^\top C = 0.
\tag{4}
$$

Then (2) *holds without control.*

2. Model description

2.1. Euler–Bernoulli beam with control and disturbance

We consider the Euler–Bernoulli beam described by

$$
\begin{aligned}
\mu \tilde{z}_{tt}(x,t) + EI\tilde{z}_{xxxx}(x,t) + c_v\tilde{z}_t(x,t) + c_k I \tilde{z}_{xxxxt}(x,t) = \\
c_a[\delta'(x-\tilde{x}_L) - \delta'(x-\tilde{x}_R)]\tilde{u}(t) + \tilde{w}(x,t), \\
\tilde{z}(0,t) = \tilde{z}_{xx}(0,t) = \tilde{z}(L,t) = \tilde{z}_{xx}(L,t) = 0,
\end{aligned}
\tag{5}
$$

where $\tilde{z} : [0,L] \times [0,\infty) \to \mathbb{R}$ is the transverse deflection of a beam of length L, linear density μ, Young's modulus of elasticity E, and moment of inertia I. The model accounts for the viscous damping $c_v\tilde{z}_t$ and structural (Kelvin–Voigt) damping $c_k I\tilde{z}_{xxxxt}$ [44,45]. The external disturbance is represented by $\tilde{w} : (0,L) \times [0,\infty) \to \mathbb{R}$. All the parameters are constant in time and space. The boundary conditions correspond to the hinged ends.

A piezoelectric actuator produces bending moment on $[\tilde{x}_L, \tilde{x}_R] \subset (0,L)$ proportional to the applied voltage $\tilde{u} : [0,\infty) \to \mathbb{R}$. Namely, $m(x,t) = c_a[h(x-\tilde{x}_L) - h(x-\tilde{x}_R)]\tilde{u}(t)$, where $h(x)$ is the step function. Since $m(x,t)$ contributes to the beam's moment–curvature relationship, it enters (5) through the Laplace operator: $m_{xx}(x,t) = c_a\delta'(x-\tilde{x}_L) - \delta'(x-\tilde{x}_R)]\tilde{u}(t)$, where $\delta'(\cdot - \tilde{x}) \in H^{-2}(0,L)$ is the derivative of the Dirac delta function defined as

$$
\delta'(\cdot - \tilde{x})f = \int_0^L \delta'(x-\tilde{x})f(x)\,dx = -f'(\tilde{x})
\tag{6}
$$

for any $\tilde{x} \in (0,L)$ and $f \in H^2(0,L)$. Note that it is natural for the derivatives of δ to be of opposite signs since the piezoelectric patch applies forces of opposite directions to its ends when it contracts or expands. A more detailed study of piezoelectric actuators is provided in [38,46,47].

Remark 2 (*Damping Model*)**.** The Kelvin–Voigt damping is motivated by the experimental observation that damping rates in beams increase with frequency [44]. This is also captured by the "square root" model given by $-c_r\tilde{z}_{xxt}$ [48]. Our analysis can be extended to the "square root" model straightforwardly.

By scaling the space and time as follows

$$
z(x,t) = \tilde{z}(a_1 x, a_2 t), \quad a_1 = \frac{L}{\pi}, \quad a_2 = a_1^2\sqrt{\frac{\mu}{EI}},
\tag{7}
$$

we rewrite (5) as

$$
\begin{aligned}
z_{tt} + z_{xxxx} + c_1 z_t + c_2 z_{xxxxt} = \left[\delta_L' - \delta_R'\right]u + w, \\
z(0,t) = z_{xx}(0,t) = z(\pi,t) = z_{xx}(\pi,t) = 0,
\end{aligned}
\tag{8}
$$

where $x \in [0,\pi]$, $t \geq 0$,

$$
c_1 = \frac{c_v a_2}{\mu}, \quad c_2 = \frac{c_k I a_2}{\mu a_1^4}, \quad x_L = \frac{\tilde{x}_L}{a_1}, \quad x_R = \frac{\tilde{x}_R}{a_1},
$$

$$
\delta_L' = \delta'\left(x - x_L\right), \quad \delta_R' = \delta'\left(x - x_R\right),
$$

$$
u(t) = \frac{c_a a_2^2}{\mu a_1^2}\tilde{u}(a_2 t), \quad w(x,t) = \frac{a_2^2}{\mu}\tilde{w}(a_1 x, a_2 t).
$$

Note that (6) implies $\delta'(a_1 x - \tilde{x}) = \delta'(x - \tilde{x}/a_1)/a_1^2$. To simplify further derivations, we assume that

$$
c_1 + c_2 \leq \sqrt{2}.
\tag{9}
$$

That is, the dynamics are dominated by the elasticity rather than damping. The extension to $c_1 + c_2 > \sqrt{2}$ is straightforward.

2.2. Well-posedness

Let H^2_{BC} and H^4_{BC} be the closure in H^2 and H^4, respectively, of all functions $f \in C^\infty[0,\pi]$ satisfying $f^{(2k)}(0) = 0 = f^{(2k)}(\pi)$ for all $k \geq 0$. The energy space of (8) is

$$
X = H^2_{BC}(0,\pi) \times L^2(0,\pi)
$$

with the scalar product

$$\langle (f_1, g_1), (f_2, g_2) \rangle_X = \langle f_1'', f_2'' \rangle_{L^2} + \langle g_1, g_2 \rangle_{L^2}.$$

Consider

$$\mathcal{A}_0 f = -f'', \quad D(\mathcal{A}_0) = H_{BC}^2(0, \pi) \subset L^2(0, \pi). \tag{10}$$

In the operator form, (8) is written as

$$\dot{\bar{z}} = \mathcal{A}\bar{z} + f, \tag{11}$$

where

$$\bar{z}(t) = \begin{bmatrix} z(\cdot, t) \\ z_t(\cdot, t) \end{bmatrix}, \quad \mathcal{A} = \begin{bmatrix} 0 & I \\ -\mathcal{A}_0^2 & -(c_1 I + c_2 \mathcal{A}_0^2) \end{bmatrix},$$

$$f(t) = \begin{bmatrix} 0 \\ [\delta_L' - \delta_R'] u(t) + w(\cdot, t) \end{bmatrix}.$$

Since $D(\mathcal{A}_0^2) = H_{BC}^4(0, \pi)$, we have

$$D(\mathcal{A}) = X_1 = H_{BC}^4(0, \pi) \times H_{BC}^4(0, \pi) \subset X.$$

The adjoint of $\mathcal{A}$ with respect to the scalar product in X is

$$\mathcal{A}^* = \begin{bmatrix} 0 & -I \\ \mathcal{A}_0^2 & -(c_1 I + c_2 \mathcal{A}_0^2) \end{bmatrix}, \quad D(\mathcal{A}^*) = X_1 \subset X.$$

Both $\mathcal{A}$ and $\mathcal{A}^*$ are dissipative. To see this, consider

$$\langle \mathcal{A}(f, g), (f, g) \rangle_X = \langle (g, -f^{(4)} - c_1 g - c_2 g^{(4)}), (f, g) \rangle_X$$
$$= \langle g'', f'' \rangle_{L^2} - \langle f^{(4)}, g \rangle_{L^2} - c_1 \langle g, g \rangle_{L^2} - c_2 \langle g^{(4)}, g \rangle_{L^2}.$$

For $f, g \in H_{BC}^4$, integration by parts gives

$$\langle f^{(4)}, g \rangle_{L^2} = \langle f'', g'' \rangle_{L^2} \quad \text{and} \quad \langle g^{(4)}, g \rangle_{L^2} = \langle g'', g'' \rangle_{L^2}.$$

Substituting, we obtain

$$\langle \mathcal{A}(f, g), (f, g) \rangle_X = -c_1 \|g\|_{L^2}^2 - c_2 \|g''\|_{L^2}^2 \leq 0.$$

Similarly,

$$\langle \mathcal{A}^*(f, g), (f, g) \rangle_X = -c_1 \|g\|_{L^2}^2 - c_2 \|g''\|_{L^2}^2 \leq 0.$$

Since $\overline{D(\mathcal{A})} = X$, $\mathcal{A}$ is closed, and $\mathcal{A}$ and $\mathcal{A}^*$ are dissipative, $\mathcal{A}$ generates a C_0-semigroup of contractions on X [49, Corollary 4.4].

The set $D(\mathcal{A}^*)$ with the norm $\|z\|_D = \|(\bar{\beta} I - \mathcal{A}^*) z\|_X$, where β is any regular point of $\mathcal{A}$ and $\bar{\beta}$ is its complex conjugate, is a Hilbert space [50, Proposition 2.10.1]. Its dual with respect to the pivot space X is $X_{-1} = Y \times H_{BC}^{-4}(0, \pi)$, where Y and H_{BC}^{-4} are the dual spaces of H_{BC}^4 with respect to H^2 and L^2, respectively.

We assume that

$$w \in H_{loc}^1((0, \infty), H_{BC}^{-4}(0, \pi)) \cap L^2((0, \infty), L^2(0, \pi)). \tag{12}$$

The control input that we design later satisfies $u \in H_{loc}^1((0, \infty), \mathbb{R})$. Since $H_{BC}^4 \subset H^2$, we have $\delta_L', \delta_R' \in H_{BC}^{-4} \supset H^{-2}$. Since δ_L' and δ_R' are constant in time, this implies

$$[\delta_L' - \delta_R'] u \in H_{loc}^1((0, \infty), H_{BC}^{-4}(0, \pi)).$$

Therefore, $f \in H_{loc}^1((0, \infty), X_{-1})$. By [50, Theorem 4.1.6], for $z(\cdot, 0) \in H_{BC}^2(0, \pi)$ and $z_t(\cdot, 0) \in L^2(0, \pi)$, there exists a unique solution of (11) in X_{-1} that satisfies

$$\bar{z} \in C([0, \infty), X) \cap C^1([0, \infty), X_{-1}).$$

Since $\bar{z} = (z, z_t)^\top$, this implies

$$z \in C([0, \infty), H_{BC}^2(0, \pi)) \quad \text{and} \quad z_t \in C([0, \infty), L^2(0, \pi)).$$

3. Robust state-feedback control of the beam

Given non-negative scalars ρ_x, ρ_u, and γ, our objective is to find a state-feedback control law guaranteeing that the trajectories of (8) with $z(\cdot, 0) \equiv 0 \equiv z_t(\cdot, 0)$ satisfy (cf. (2))

$$J = \int_0^\infty \left[\|z(\cdot, t)\|^2 + \rho_x \|z_{xx}(\cdot, t)\|^2 + \rho_u u^2(t) - \gamma^2 \|w(\cdot, t)\|^2 \right] dt \leq 0 \tag{13}$$

for all w satisfying (12). Such control guarantees that the L^2 gain is not greater than γ. Using (7), one can rewrite (13) in terms of the original state, input, and disturbance with $\tilde{\rho}_x = \rho_x a_1^4$, $\tilde{\rho}_u = \rho_u \frac{c_a^2 a_2^4}{\mu^2 a_1^3}$, and $\tilde{\gamma} = \gamma \frac{a_2^2}{\mu}$.

Remark 3 (*Performance Index*). Since the potential energy of (5) due to bending is $\frac{EI}{2} \|\bar{z}_{xx}(\cdot, t)\|^2$ [51, p. 317], we include $\|z_{xx}(\cdot, t)\|^2$ in (13). The kinetic energy of (5) is $\frac{\mu}{2} \|\bar{z}_t(\cdot, t)\|^2$, and it is natural to include $\|z_t(\cdot, t)\|^2$ in (13). To simplify the exposition, we do not present this extension, which requires one to consider multiple cases depending on the values of c_1, c_2, ρ_x, and ρ_u.

3.1. Modal decomposition

The modes and natural frequencies of (8) are

$$\varphi_n(x) = \sqrt{2/\pi} \sin nx, \quad \omega_n = n^2, \quad n \in \mathbb{N}.$$

These are the eigenfunctions and eigenvalues of $\mathcal{A}_0$ defined in (10), which form a complete orthonormal system in $L^2(0, \pi)$. Therefore,

$$z(\cdot, t) \overset{L^2}{=} \sum_{n=1}^\infty z_n(t) \varphi_n, \quad z_n(t) = \langle z(\cdot, t), \varphi_n \rangle.$$

Substituting this into (8), in view of

$$\langle \delta_L', \varphi_n \rangle \overset{(6)}{=} -\varphi_n'(x_L) \quad \text{and} \quad \langle \delta_R', \varphi_n \rangle \overset{(6)}{=} -\varphi_n'(x_R),$$

we obtain the ODEs for the Fourier coefficients

$$\ddot{z}_n(t) + 2\zeta_n \omega_n \dot{z}_n(t) + \omega_n^2 z_n(t) = b_n u(t) + w_n(t), \quad n \in \mathbb{N},$$

where

$$\zeta_n = (c_1 \omega_n^{-1} + c_2 \omega_n)/2,$$
$$b_n = n\sqrt{2/\pi} \left(\cos nx_R - \cos nx_L \right),$$
$$w_n(t) = \langle w(\cdot, t), \varphi_n \rangle.$$

The ODEs can be written as

$$\dot{\bar{z}}_n(t) = A_n \bar{z}_n(t) + B_n u(t) + E_n w_n(t), \quad n \in \mathbb{N}, \tag{14}$$

where

$$\bar{z}_n = \begin{bmatrix} z_n \\ \dot{z}_n \end{bmatrix}, \quad A_n = \begin{bmatrix} 0 & 1 \\ -\omega_n^2 & -2\zeta_n \omega_n \end{bmatrix}, \quad B_n = \begin{bmatrix} 0 \\ b_n \end{bmatrix}, \quad E_n = \begin{bmatrix} 0 \\ 1 \end{bmatrix}.$$

The eigenvalues of A_n are

$$\lambda_n^{\mp} = -\omega_n(\zeta_n \pm \sqrt{\zeta_n^2 - 1}). \tag{15}$$

Without damping ($\zeta_n = 0$), infinitely many imaginary roots $\lambda_n^\pm = \pm i\omega_n$ (see Fig. 1) give rise to free vibrations in (8) in the absence of control and disturbance. Our approach does not work in this case since it is not enough to deal only with a finite number of modes. Viscous damping ($c_1 \neq 0$) ensures that $\text{Re}\,\lambda_n^\pm = -c_1/2$. Kelvin–Voigt damping ($c_2 \neq 0$) improves the stability further guaranteeing

$$\text{Re}\,\lambda_n^- \to -\infty \quad \text{and} \quad \text{Re}\,\lambda_n^+ \to -1/c_2.$$

We develop our approach for the case when $c_1 \neq 0 \neq c_2$.

3.2. The spillover phenomenon

It is common in engineering practice to design controllers based on a few dominating modes while ignoring the residue. This subsection demonstrates that such an approach may suffer from the spillover phenomenon.

Consider the Euler–Bernoulli beam (8) with

$$c_1 = 1.4 \times 10^{-3}, \ c_2 = 1.3 \times 10^{-3}, \ x_L = 0.91, \ x_R = 0.97.$$

The choice of the parameters is explained in Section 4. Let us try to design a controller guaranteeing (13) with $\rho_x = 0.1$ and $\rho_u = 10^{-3}$ by considering only 5 modes in the modal decomposition (14). Using
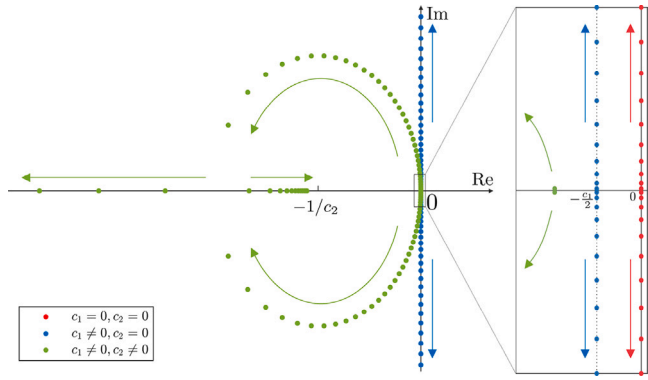
Fig. 1. The eigenvalues of A_n given in (15) for $n = 1, \ldots, 50$. Red dots — no damping ($c_1 = 0 = c_2$); blue dots — viscous damping ($c_1 = 1.4 \times 10^{-3}$, $c_2 = 0$); green dots — viscous and Kelvin–Voigt damping ($c_1 = 1.4 \times 10^{-3}$, $c_2 = 1.3 \times 10^{-3}$). (For interpretation of the references to color in this figure legend, the reader is referred to the web version of this article.)
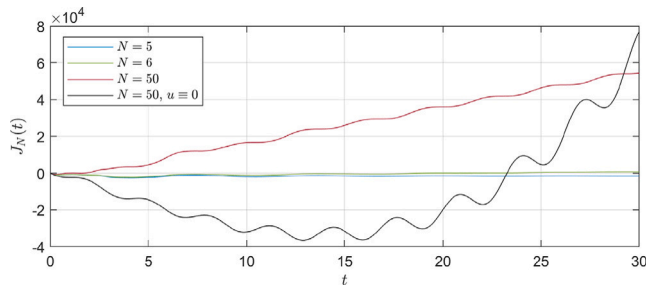

Fig. 2. The value of $J_N(t)$, defined in (16), for $N = 5$ (blue), $N = 6$ (green), and $N = 50$ (red). The black line is $J_N(t)$ for $N = 50$ and $u \equiv 0$. A controller designed for the first 5 modes cannot guarantee (13) for the original system because of the spillover phenomenon. (For interpretation of the references to color in this figure legend, the reader is referred to the web version of this article.)

Proposition 1 (see Section 3.5 for details), we find $\gamma \approx 6.97$ and the corresponding controller gain $-R^{-1}B^\top P \in \mathbb{R}^{1 \times 10}$.

Fig. 2 shows the values of

$$J_N(t) = \int_0^t \left[\sum_{n=1}^{N} \left[(1 + \rho_x \omega_n^2) z_n^2(t) - \gamma^2 w_n^2(t) \right] + \rho_u u^2(t) \right] dt \quad (16)$$

for different numbers of modes, N. Proposition 1 guarantees $J_5(t) \leq 0$ (blue line). However, if we include one more mode without adjusting γ and the controller, then

$$J_6(t) = J_5(t) + \int_0^t \left[(1 + \rho_x \omega_6^2) z_6^2(t) - \gamma^2 w_6^2(t) \right] dt$$

becomes positive for $t > 20$ (green line). This happens because the L^2 gain for the additional mode with $n = 6$ is greater than γ and the additional integral term is positive. The red line shows $J_{50}(t) \approx J_\infty(t)$, which is the cost when all the modes are considered. Clearly, the controller designed using only 5 modes cannot guarantee (13) for the original system.

Spillover occurs because the effect of the controller on the truncated modes is ignored. In the remainder of the paper, we provide a simple remedy to avoid spillover. Namely, we show how to modify ρ_u in (16) so that a controller guaranteeing $J_N(t) \leq 0$ for a given N will guarantee (13) with the original ρ_u.

3.3. Cost decomposition

We represent (14) as

$$\dot{z}^N = Az^N + Bu + Ew^N, \quad (17a)$$

$$\dot{\bar{z}}_n = A_n \bar{z}_n + B_n u + E_n w_n, \quad n > N, \quad (17b)$$

where $N \in \mathbb{N}$,

$$z^N = \begin{bmatrix} z_1 \\ \vdots \\ z_N \\ \dot{z}_1 \\ \vdots \\ \dot{z}_N \end{bmatrix}, \quad w^N = \begin{bmatrix} w_1 \\ \vdots \\ w_N \end{bmatrix}, \quad B = \begin{bmatrix} 0 \\ \vdots \\ 0 \\ b_1 \\ \vdots \\ b_N \end{bmatrix}, \quad E = \begin{bmatrix} 0_N \\ I_N \end{bmatrix}, \quad (18)$$

$$A = \begin{bmatrix} 0_N & I_N \\ -\Omega_N^2 & -\left(c_1 I_N + c_2 \Omega_N^2 \right) \end{bmatrix}, \quad \Omega_N = \mathrm{diag}\{\omega_1, \ldots, \omega_N\},$$

and the remaining notations are from (14). We will design an H_∞ controller for (17a) with the cost, J_0, that accounts for its effect on (17b). To find this cost, we decompose the original cost J from (13). Namely, since $z(\cdot, t) \in H^2(0, \pi)$ (see Section 2.2), Parseval's identity gives

$$\|z(\cdot, t)\|^2 = \sum_{n=1}^{\infty} z_n^2(t), \quad \|z_{xx}(\cdot, t)\|^2 = \sum_{n=1}^{\infty} \omega_n^2 z_n^2(t).$$

Our key idea is to represent J from (13) as

$$J = J_0 + \sum_{n=N+1}^{\infty} J_n, \quad (19)$$

where

$$J_0 = \int_0^\infty \left[\sum_{n=1}^{N} (1 + \rho_x \omega_n^2) z_n^2(t) + \left(\rho_u + \sum_{n=N+1}^{\infty} \rho_n \right) u^2(t) - \gamma^2 \sum_{n=1}^{N} w_n^2(t) \right] dt,$$

$$J_n = \int_0^\infty \left[(1 + \rho_x \omega_n^2) z_n^2(t) - \rho_n u^2(t) - \gamma^2 w_n^2(t) \right] dt.$$

The control, $u(t)$, is treated as a disturbance in (17b). Using the bounded real lemma (Corollary 1), we will find the minimum ρ_n such that $J_n \leq 0$ for the zero initial conditions and any $w_n \in L^2([0, \infty), \mathbb{R})$. Then, we will show that $\sum_{n=N+1}^{\infty} \rho_n < \infty$ and construct a controller for (17a) guaranteeing $J_0 \leq 0$.

3.4. Bounded real lemma for the residue

For a given $n > N$, (17b) can be represented as (1) with

$$x = \bar{z}_n, \quad A = A_n, \quad B = 0_{2 \times 1}, \quad v = \begin{bmatrix} \sqrt{\rho_n} u / \gamma \\ w_n \end{bmatrix}, \quad E = \begin{bmatrix} \frac{\gamma}{\sqrt{\rho_n}} B_n & E_n \end{bmatrix}.$$

Note that the control input, u, is considered as a part of the disturbance, v, since the H_∞ control will be designed based on (17a). The cost in (2) coincides with J_n for

$$C = \begin{bmatrix} \sqrt{1 + \rho_x \omega_n^2} & 0 \end{bmatrix} \quad \text{and} \quad D = 0.$$

Then, the algebraic Riccati Eq. (4) takes the form

$$P_n A_n + A_n^\top P_n + \gamma^{-2} P_n \begin{bmatrix} 0 & 0 \\ 0 & 1 + \gamma^2 b_n^2 / \rho_n \end{bmatrix} P_n + \begin{bmatrix} 1 + \rho_x \omega_n^2 & 0 \\ 0 & 0 \end{bmatrix} = 0. \quad (20)$$

In Appendix A, we show that the smallest ρ_n guaranteeing the feasibility of (20) is

$$\rho_n = \begin{cases} \dfrac{b_n^2(1 + \rho_x \omega_n^2)}{4\omega_n^4 \zeta_n^2(1 - \zeta_n^2) - (1 + \rho_x \omega_n^2)\gamma^{-2}} & \text{if } 2\zeta_n^2 \leq 1, \\[3ex] \dfrac{b_n^2(1 + \rho_x \omega_n^2)}{\omega_n^4 - (1 + \rho_x \omega_n^2)\gamma^{-2}} & \text{if } 2\zeta_n^2 > 1. \end{cases}$$

The value of ρ_n is the L^2 gain from u to $\bar{z}_n$. Corollary 1 guarantees $J_n \leq 0$ for these ρ_n. This can be used to obtain the L^2 gain of (8) without control.

Proposition 2 (L^2 *Gain without Control*). *The L^2 gain of the control-free (8) subject to (9) is not greater than*

$$\gamma_0 = \frac{2\sqrt{1 + \rho_x}}{(c_1 + c_2)\sqrt{4 - (c_1 + c_2)^2}}.$$

Proof. Repeating the arguments of Appendix A with $\alpha_n = \gamma^{-2}$, we obtain that (20) is feasible for any $n \in \mathbb{N}$ if

$$\gamma^2 \geq \frac{1 + \rho_x \omega_n^2}{4\omega_n^4 \zeta_n^2(1 - \zeta_n^2)} \quad \text{when} \quad 2\zeta_n^2 \leq 1, \quad (21a)$$

$$\gamma^2 \geq \frac{1 + \rho_x \omega_n^2}{\omega_n^4} \quad \text{when} \quad 2\zeta_n^2 > 1. \tag{21b}$$

The right-hand sides of (21) are decreasing in n. Moreover,

$$\omega_n^4 - 4\omega_n^4 \zeta_n^2 (1 - \zeta_n^2) = \omega_n^4 (1 - 2\zeta_n^2)^2 \geq 0$$

implies that the bound in (21a) is not smaller than in (21b). Since (9) guarantees $2\zeta_1^2 \leq 1$, the lower bound on γ is obtained from (21a) with $n = 1$, i.e., with $\omega_1 = 1$ and $\zeta_1 = (c_1 + c_2)/2$. The feasibility of (20) implies $J_n \leq 0$. Taking $N = 0$ and $J_0 = 0$ in (19), we obtain $J \leq 0$. □

In Appendix B, we show that

$$\sum_{n=N+1}^{\infty} \rho_n \leq \rho_\infty = \sum_{n=N+1}^{M} \rho_n + C_M \left[|x_R - x_L| - \sum_{n=1}^{M} \frac{b_n^2}{\omega_n^2} \right], \tag{22}$$

where

$$C_M = \frac{\omega_{M+1}^2 (1 + \rho_x \omega_{M+1}^2)}{\omega_{M+1}^4 - (1 + \rho_x \omega_{M+1}^2)\gamma^{-2}},$$

$$M = \max \left\{ N, \left\lfloor \sqrt{\frac{1 + \sqrt{1 - 2c_1 c_2}}{\sqrt{2}c_2}} \right\rfloor \right\}.$$

Here, $\lfloor \cdot \rfloor$ stands for the integer part. Note that (9) implies $2c_1 c_2 \leq 1$.

As explained in Appendix B, $\sum_{n=1}^{\infty} b_n^2/\omega_n^2 = |x_R - x_L|$. Therefore, $\rho_\infty \to 0$ monotonically as $N \to \infty$. That is, by considering more modes in the control design, we reduce the L^2 gain of the residue associated with the spillover.

3.5. H_∞ controller design without spillover

The system (17a) is in the form of (1) with $x = z^N$, $v = w^N$, and A, B, and E defined in (18). Taking

$$C = \begin{bmatrix} \sqrt{I_N + \rho_x \Omega_N^2} & 0_{N \times N} \\ 0_{1 \times N} & 0_{1 \times N} \end{bmatrix} \quad \text{and} \quad D = \begin{bmatrix} 0_{N \times 1} \\ \sqrt{\rho_u + \rho_\infty} \end{bmatrix}, \tag{23}$$

we obtain that $D^\top C = 0$, $R = D^\top D = \rho_u + \rho_\infty > 0$, and the left-hand side of (2) coincides with J_0 from (19). By Proposition 1, if $0 < P \in \mathbb{R}^{2N \times 2N}$ satisfies (3), then

$$u(t) = -(\rho_u + \rho_\infty)^{-1} B^\top P z^N(t) \tag{24}$$

guarantees $J_0 \leq 0$. Since ρ_n were chosen so that $J_n \leq 0$, we obtain that $J \leq 0$.

Note that (12) implies $w^N \in L^2(0, \infty)$. Therefore, the solution of the stable system (17a), (24) satisfies $z^N \in L^2(0, \infty)$. That is, the right-hand side of (17a) is from L^2, meaning that $\dot{z}^N \in L^2(0, \infty)$, and both $z^N \in H^1(0, \infty)$ and $u \in H^1(0, \infty)$. This is the property we used in the well-posedness analysis of Section 2.2. Summarizing, we have the following result.

Theorem 1. *Consider the Euler–Bernoulli beam (8) subject to (9) and its modal decomposition (17) with some $N \in \mathbb{N}$. Given non-negative ρ_x, ρ_u, and γ, let ρ_∞ be given by (22). If $0 < P \in \mathbb{R}^{2N \times 2N}$ satisfies the algebraic Riccati Eq. (3) with A, B, C, D, and E given in (18) and (23), then the state feedback (24) guarantees that the L^2 gain of (8) is not greater than γ, that is, (13) holds for $z(\cdot, 0) \equiv 0 \equiv z_t(\cdot, 0)$ and any w satisfying (12).*

Proof. Let M be as defined below (22). Consider

$$V = (z^N)^\top P z^N + \sum_{n=N+1}^{\infty} \bar{z}_n^\top P_n \bar{z}_n$$

with P_n defined by (A.3) for $N + 1 \leq n \leq M$ and by (A.4) for $n > M$. The series converges since

$$P_n \sim \rho_x \begin{bmatrix} \omega_n^2 c_2 & 1 \\ 1 & 2c_2 \end{bmatrix} \quad \text{as} \quad n \to \infty \tag{25}$$

(we chose "+" for the right bottom element), while $z(\cdot, t) \in H^2(0, \pi)$ and $z_t(\cdot, t) \in L^2(0, \pi)$ (see Section 2.2). Let $J(t)$ be J as defined in (13) but with ∞ replaced by t. Calculating the derivative along the

trajectories of (17) and using the relation $\rho_u + \sum_{N+1}^{\infty} \rho_n \leq \rho_u + \rho_\infty = R$, we obtain

$$\dot{V}(t) + \dot{J}(t) \leq 2(z^N)^\top P[Az^N + Bu + Ew^N]$$
$$+ (z^N)^\top C^\top C z^N + Ru^2 - \gamma^2 |w^N|^2$$
$$+ 2\sum_{n=N+1}^{\infty} \bar{z}_n^\top P_n [A_n \bar{z}_n + B_n u + E_n w_n]$$
$$+ \sum_{n=N+1}^{\infty} [(1 + \rho_x \omega_n^2) z_n^2 - \rho_n u^2 - \gamma^2 w_n^2].$$

Completing the squares, we find

$$2(z^N)^\top P Bu + Ru^2 = |R^{-\frac{1}{2}} B^\top P z^N + R^{\frac{1}{2}} u|^2 - (z^N)^\top PBR^{-1}B^\top P z^N,$$
$$2(z^N)^\top P Ew^N - \gamma^2 |w^N|^2 = \gamma^{-2}|E^\top P z^N|^2 - |\gamma^{-1} E^\top P z^N - \gamma w^N|^2, \tag{26}$$
$$2\bar{z}_n^\top P_n B_n u - \rho_n u^2 = \rho_n^{-1}|B_n^\top P_n \bar{z}_n|^2 - |\rho_n^{-\frac{1}{2}} B_n^\top P_n \bar{z}_n - \rho_n^{\frac{1}{2}} u|^2,$$
$$2\bar{z}_n^\top P_n E_n w_n - \gamma^2 w_n^2 = \gamma^{-2}|E_n^\top P_n \bar{z}_n|^2 - |\gamma^{-1} E_n^\top P_n \bar{z}_n - \gamma w_n|^2.$$

In view of (3) and (20), these lead to

$$\dot{V}(t) + \dot{J}(t) \leq |R^{-\frac{1}{2}} B^\top P z^N + R^{\frac{1}{2}} u|^2 - |\gamma^{-1} E^\top P z^N - \gamma w^N|^2$$
$$- \sum_{n=N+1}^{\infty} \left[|\rho_n^{-\frac{1}{2}} B_n^\top P_n \bar{z}_n - \rho_n^{\frac{1}{2}} u|^2 + |\gamma^{-1} E_n^\top P_n \bar{z}_n - \gamma w_n|^2 \right].$$

Substituting u from (24), we obtain

$$\dot{V}(t) + \dot{J}(t) \leq 0. \tag{27}$$

Integrating the above from 0 to t, we obtain

$$V(t) - V(0) + J(t) - J(0) \leq 0.$$

Given that $V(0) = 0$ for the zero initial conditions, and $J(0) = 0$, we have $J(t) \leq -V(t) \leq 0$, which implies (13). □

Remark 4 (*Internal Stability*). The designed feedback (24) renders (8) internally stable in the norm

$$\|z(\cdot, t)\|_X^2 = \|z_{xx}(\cdot, t)\|^2 + \|z_t(\cdot, t)\|^2.$$

Indeed, (25) implies the existence of positive ε_1 and ε_2 such that $\varepsilon_1 \|z(\cdot, t)\|_X^2 \leq V \leq \varepsilon_2 \|z(\cdot, t)\|_X^2$, and (27) implies $\dot{V} \leq 0$ for $w(\cdot, t) \equiv 0$.

Remark 5 (*Solution Existence*). Since A, defined in (18), is Hurwitz, (A, B) is stabilizable. It is easy to check that (A, C) is observable, hence detectable. As mentioned in Remark 1, this guarantees that (3) has a solution for a large enough γ. That is, the conditions of Theorem 1 hold for any $N \in \mathbb{N}$ and large enough γ.

Remark 6 (*Number of Modes and the L^2 Gain*). When N grows, γ can only decrease. Indeed, we know that $J_{N+1}(t) \leq 0$ and (24) guarantees $J_0(t) \leq 0$ with $J_{N+1}(t)$ and $J_0(t)$ defined below (19). Taking $K_1, K_2 \in \mathbb{R}^{1 \times N}$ such that $[K_1 \ K_2] = (\rho_u + \rho_\infty)^{-1} B^\top P$, we have that

$$u = - \begin{bmatrix} K_1 & 0 & K_2 & 0 \end{bmatrix} z^{N+1}$$

guarantees $\bar{J}_0(t) = J_0(t) + J_{N+1}(t) \leq 0$. Note that $\bar{J}_0(t)$ is $J_0(t)$ with N replaced by $N + 1$. By [2, Theorem 6.3.6], (3) has a solution for the matrices defined in (18) and (23) with N replaced by $N + 1$. That is, the same γ is achievable with $N + 1$ modes. When considering $N + 1$ modes, we are making the sum $J_0(t) + J_{N+1}(t)$ negative instead of each term, $J_0(t)$ and $J_{N+1}(t)$, independently. This gives more flexibility and may reduce γ, as demonstrated in Fig. 3.

4. Numerical simulations

As an example, we consider an aluminum rectangular beam of dimensions $1\,\text{m} \times 0.1\,\text{m} \times 0.01\,\text{m}$ with hinged ends and a piezoelectric actuator of length $2\,\text{cm}$ placed at $30\,\text{cm}$ from the left edge. This system can be modeled by (5) with the parameters given in the following table:
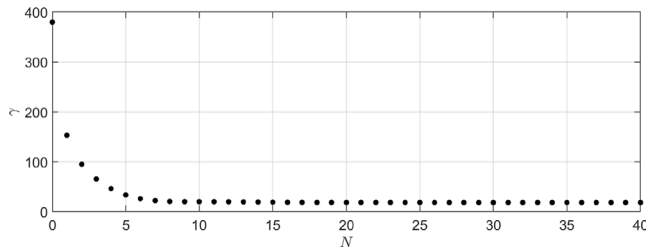
Fig. 3. The L^2 gain of the Euler–Bernoulli beam (8) for different numbers of controlled modes N.

Linear density	μ	2.71 kg/m
Young's modulus	E	70×10^9 N/m^2
Moment of inertia	I	8.3×10^{-8} m^4
Viscous damping	c_v	1.76 kg/(m s)
Structural damping	c_k	2.05×10^5 kg/(m s)
Left actuator position	$\tilde{x}_L$	0.29 m
Right actuator position	$\tilde{x}_R$	0.31 m

The linear density is calculated as $\mu = \rho A$, where $\rho = 2710$ kg/m^3 is the density of aluminum, and $A = 0.1 \times 0.01 = 10^{-3}$ m^2 is the cross-section area of the beam. The damping coefficients, c_v and c_k, are taken from [52]. The value of c_a depends on the type of the piezoelectric patch; it does not affect the performance analysis since the control can be scaled as $\tilde{u}' = c_a \tilde{u}$. After the change of variables (7), we obtain (8) with

$$c_1 = 1.4 \times 10^{-3}, \quad c_2 = 1.3 \times 10^{-3}, \quad x_L = 0.91, \quad x_R = 0.97.$$

Our objective is to design a state-feedback control law of the form (24) guaranteeing that the solution of (8) with $z(\cdot, 0) \equiv 0 \equiv z_t(\cdot, 0)$ satisfies (13) with $\rho_u = 10^{-3}$, $\rho_x = 0.1$, and smallest possible $\gamma > 0$. To decide on how many modes to consider in the controller design, we calculate the minimum γ for different numbers of controlled modes, N. Proposition 2 gives $\gamma_0 \approx 380$ as the smallest L^2 gain without control. For each integer $N \in [1, 40]$, we found the minimum γ satisfying the conditions of Theorem 1. The results are shown in Fig. 3. As explained in Remark 6, the L^2 gain decreases when more modes are considered. The limit value is $\gamma \approx 18$. Since γ does not improve significantly for $N > 8$, we consider $N = 8$ modes. In this case, $\gamma \approx 20.2$ and $\rho_\infty \approx 8 \times 10^{-3}$, which we found using (22). To find the controller gain in (24), we solve (3) for $P > 0$ with A, B, C, D, and E defined in (18) and (23). Note that, for this example, the first condition in (15) of [35] requires $N \geq 32$ and the resulting LMIs are not feasible for any $\gamma > 0$.

The results of numerical simulations without and with control for the same disturbance are shown in Fig. 4. To generate the disturbance, we calculated $P > 0$ satisfying (4) with A, E, and C given in (18) and (23), found $z_d^N(t)$ as the solution of (17a) with $N = 30$, $u \equiv 0$, and $z_d^N(0) = [1, \ldots, 1]^\top \in \mathbb{R}^{60}$, substituted $w^N(t) = \gamma^{-2} E^\top P z_d^N(t)$ into (18), and took $w(x, t) = \sum_{n=1}^N w_n(t) \varphi_n(x)$. The value of w^N was selected to maximizes the related negative term in (26). Clearly, the proposed control strategy attenuates the effect of the disturbance. This is also evident from Fig. 5, which shows

$$\|z(\cdot, t)\|_J = \sqrt{\|z(\cdot, t)\|^2 + \rho_x \|z_{xx}(\cdot, t)\|^2} \tag{28}$$

without (black) and with (blue) control.

The value of $J(t)$, obtained by replacing ∞ with t in (13), is shown in Fig. 6. As guaranteed by Theorem 1, the control ensures that $J = \lim_{t \to \infty} J(t) < 0$ for $\gamma \approx 20.2$ (blue line). Without control (black line), $J(t)$ becomes positive for $t \approx 70$. If the residue is ignored ($\rho_\infty = 0$), a smaller $\gamma \approx 7.16$ is obtained following the steps detailed in Section 3.2. In this case, the spillover phenomenon causes $J(t) > 0$ for $t > 7$ (red line). This vividly demonstrates why the residue, i.e., the modes with $n > N$, must not be ignored. Theorem 1 provides a simple way of designing a controller avoiding the spillover phenomenon.
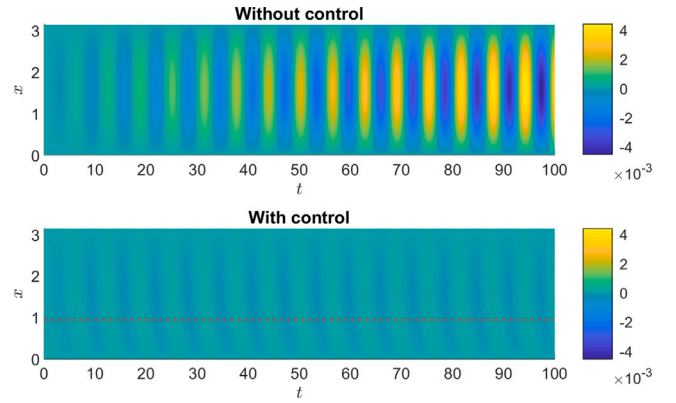

Fig. 4. Euler–Bernoulli beam without and with control. The red dashed lines show the ends of the piezoelectric actuator.
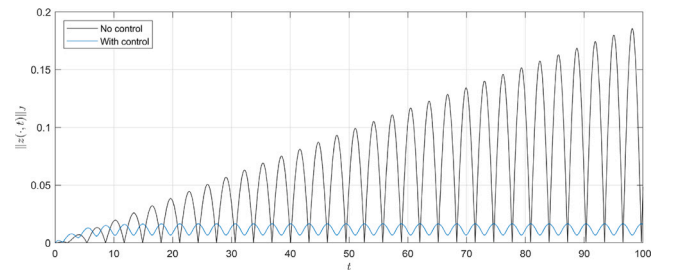

Fig. 5. The value of $\|z(\cdot, t)\|_J$, defined in (28), without (black) and with (blue) control. (For interpretation of the references to color in this figure legend, the reader is referred to the web version of this article.)
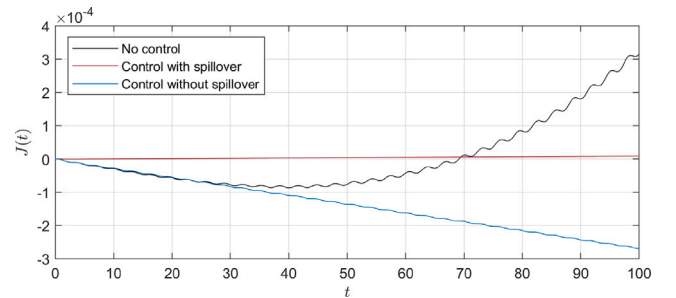

Fig. 6. The value of $J(t)$ (given by (13) with ∞ replaced by t) without control (black) and with control (blue) for $\gamma \approx 20.2$. The red line shows the spillover phenomenon occurring when the modes with $n > 8$ are ignored. (For interpretation of the references to color in this figure legend, the reader is referred to the web version of this article.)

Remark 7 (*N vs γ with spillover*)**.** If the residue is ignored ($\rho_\infty = 0$), then $\gamma \approx 6.97$ for $N = 5$ (see Section 3.2) and $\gamma \approx 7.16$ for $N = 8$ (as explained above). That is, the L^2 gain may increase when more modes are considered. This happens because, by increasing N, one obtains a more accurate estimate of the actual L^2 gain, which is larger than that obtained using the truncated modal decomposition. If the residue is accounted for, larger N will never lead to a larger γ (see Remark 6).

5. Conclusions

We studied the H_∞ control of the Euler–Bernoulli beam with viscous and Kelvin–Voigt damping using piezoelectric actuators. We showed that spillover occurs when a finite number of modes are considered in the H_∞ design. Then we proposed a simple modification of the cost guaranteeing that the controller designed based on a finite number of modes does not lead to spillover. Using a realistic model of the beam,

we demonstrated how to find the number of modes required to design a controller, i.e., such that a further increase of the number of considered modes does not improve the L^2 gain significantly.

CRediT authorship contribution statement

Anton Selivanov: Writing – review & editing, Writing – original draft, Visualization, Methodology, Investigation, Formal analysis, Conceptualization. **Emilia Fridman:** Conceptualization.

Declaration of competing interest

The authors declare the following financial interests/personal relationships which may be considered as potential competing interests: Emilia Fridman reports financial support was provided by ISF-NSFC Joint Research Program. Emilia Fridman reports financial support was provided by C. and H. Manderman Chair at Tel Aviv University. If there are other authors, they declare that they have no known competing financial interests or personal relationships that could have appeared to influence the work reported in this paper.

Acknowledgments

Appendix A. Solution of (20)

Let $P_n = \begin{bmatrix} p_1 & p_2 \\ p_2 & p_3 \end{bmatrix}$. Then (20) is equivalent to

$$\alpha_n p_2^2 - 2\omega_n^2 p_2 + (1 + \rho_x \omega_n^2) = 0,$$
$$p_1 - 2\zeta_n \omega_n p_2 - p_3 \omega_n^2 + \alpha_n p_2 p_3 = 0,$$
$$\alpha_n p_3^2 - 4\zeta_n \omega_n p_3 + 2p_2 = 0$$

with $\alpha_n = b_n^2/\rho_n + \gamma^{-2}$. These are equivalent to

$$
\begin{aligned}
p_2 &= \alpha_n^{-1}\left[\omega_n^2 \pm \sqrt{\omega_n^4 - \alpha_n(1 + \rho_x \omega_n^2)}\right], \\
p_3 &= \alpha_n^{-1}\left[2\zeta_n \omega_n \pm \sqrt{4\zeta_n^2 \omega_n^2 - 2\alpha_n p_2}\right], \\
p_1 &= 2\zeta_n \omega_n p_2 + p_3 \omega_n^2 - \alpha_n p_2 p_3.
\end{aligned}
\tag{A.1}
$$

These values are real if and only if

$$\omega_n^4 \geq \alpha_n(1 + \rho_x \omega_n^2) \quad \text{and} \tag{A.2a}$$

$$2\zeta_n^2 \omega_n^2 \geq \alpha_n p_2 = \omega_n^2 - \sqrt{\omega_n^4 - \alpha_n(1 + \rho_x \omega_n^2)}. \tag{A.2b}$$

We took p_2 with "−" since $2\zeta_n^2$ can be smaller than 1.

To minimize ρ_n, we maximize α_n. If $2\zeta_n^2 < 1$, then (A.2b) gives the maximum $\alpha_n = 4\omega_n^4 \zeta_n^2(1 - \zeta_n^2)/(1 + \rho_x \omega_n^2)$, which satisfies (A.2a) since $\omega_n^4 - \alpha_n(1 + \rho_x \omega_n^2) = \omega_n^4(1 - 2\zeta_n^2)^2 > 0$. Substituting this into (A.1), we obtain

$$P_n = \frac{2\zeta_n \omega_n}{\alpha_n}\begin{bmatrix} \omega_n^2 & \zeta_n \omega_n \\ \zeta_n \omega_n & 1 \end{bmatrix} > 0. \tag{A.3}$$

If $2\zeta_n^2 \geq 1$, then (A.2b) is true subject to (A.2a), which gives $\alpha_n = \omega_n^4/(1 + \rho_x \omega_n^2)$. Substituting this into (A.1), we obtain

$$P_n = \frac{\omega_n}{\alpha_n}\begin{bmatrix} 2\zeta_n \omega_n^2 & \omega_n \\ \omega_n & 2\zeta_n \pm \sqrt{4\zeta_n^2 - 2} \end{bmatrix} > 0. \tag{A.4}$$

The minimum values of ρ_n are calculated from $\alpha_n = b_n^2/\rho_n + \gamma^{-2}$ with the corresponding α_n.

Appendix B. Upper bound on the L^2 gain for the residue

For $n > M$, we have $\zeta_n \geq 1/\sqrt{2}$. Then

$$
\begin{aligned}
\rho_n &= \frac{b_n^2(1 + \rho_x \omega_n^2)}{\omega_n^4 - (1 + \rho_x \omega_n^2)\gamma^{-2}} = \frac{\omega_n^{-2} + \rho_x}{1 - (\omega_n^{-2} + \rho_x)\omega_n^{-2}\gamma^{-2}}\frac{b_n^2}{\omega_n^2} \\
&\leq \frac{\omega_{M+1}^{-2} + \rho_x}{1 - (\omega_{M+1}^{-2} + \rho_x)\omega_{M+1}^{-2}\gamma^{-2}}\frac{b_n^2}{\omega_n^2} = C_M \frac{b_n^2}{\omega_n^2}.
\end{aligned}
$$

Note that b_n/ω_n are the Fourier coefficients of

$$\chi_{[x_L, x_R]}(x) = \begin{cases} 1, & x \in [x_L, x_R], \\ 0, & x \notin [x_L, x_R]. \end{cases}$$

By Parseval's identity,

$$\sum_{n=1}^{\infty} \frac{b_n^2}{\omega_n^2} = \|\chi_{[x_L, x_R]}\|^2 = |x_R - x_L|.$$

Therefore,

$$\sum_{n=M+1}^{\infty} \rho_n \leq C_M \sum_{n=M+1}^{\infty} \frac{b_n^2}{\omega_n^2} = C_M\left[|x_R - x_L| - \sum_{n=1}^{M} \frac{b_n^2}{\omega_n^2}\right],$$

which implies (22).

Data availability

No data was used for the research described in the article.

References

[1] B.A. Francis (Ed.), A course in H-infinity control theory, in: Lecture Notes in Control and Information Sciences, vol. 88, Springer-Verlag, Berlin/Heidelberg, 1987.

[2] M. Green, D. Limebeer, Linear Robust Control, Dover Books on Electrical Engineering, Dover Publications, Incorporated, 2012.

[3] H. Özbay, A. Tannenbaum, A skew toeplitz approach to the H-infinity optimal control of multivariable distributed systems, SIAM J. Control Optim. 28 (3) (1990) 653–670.

[4] H. Özbay, H-infinity optimal controller design for a class of distributed parameter systems, Internat. J. Control 58 (4) (1993) 739–782.

[5] C.N. Nett, C.A. Jacobson, M.J. Balas, Fractional representation theory: Robustness results with applications to finite dimensional control of a class of linear distributed systems, in: The 22nd IEEE Conference on Decision and Control, 1983, pp. 268–280.

[6] K. Glover, Robust stabilization of linear multivariable systems: Relations to approximation, Internat. J. Control 43 (3) (1986) 741–766.

[7] H. Özbay, A. Tannenbaum, On the structure of suboptimal H-infinity controllers in the sensitivity minimization problem for distributed stable plants, Automatica 27 (2) (1991) 293–305.

[8] J. Bontsema, R.F. Curtain, A note on spillover and robustness for flexible systems, IEEE Trans. Autom. Control 33 (6) (1988) 567–569.

[9] R.F. Curtain, H. Zwart, An Introduction to Infinite-Dimensional Linear Systems Theory, Springer, New York, 1995, p. 21.

[10] R. Curtain, H-infinity control for distributed parameter systems: A survey, in: 29th IEEE Conference on Decision and Control, 1990, pp. 22–26.

[11] B. van Keulen, H-Infinity-Control for Distributed Parameter Systems: A State-Space Approach, Birkhäuser, Boston, 1993.

[12] M. Athans, Toward a practical theory for distributed parameter systems, IEEE Trans. Autom. Control 15 (2) (1970) 245–247.

[13] M.J. Balas, Toward a more practical control theory for distributed parameter systems, in: C. Leondes (Ed.), Advances in Theory and Applications, Academic Press, 1982, pp. 18, 361–421.

[14] R. Triggiani, Boundary feedback stabilizability of parabolic equations, Appl. Math. Optim. 6 (1) (1980) 201–220.

[15] M.J. Balas, Trends in large space structure control theory: Fondest hopes, wildest dreams, IEEE Trans. Autom. Control. 27 (3) (1982) 522–535.

[16] R.F. Curtain, A Comparison of Finite-Dimensional Controller Designs for Distributed Parameter Systems, Research Report RR-1647, Inria, 1992.

[17] M.J. Balas, Feedback control of flexible systems, IEEE Trans. Autom. Control 23 (4) (1978) 673–679.

[18] L. Meirovitch, H. Baruh, On the problem of observation spillover in self-adjoint distributed-parameter systems, J. Optim. Theory Appl. 39 (2) (1983) 269–291.

[19] M.J. Balas, Finite-dimensional controllers for linear distributed parameter systems: Exponential stability using residual mode filters, J. Math. Anal. Appl. 133 (2) (1988) 283–296.

[20] S.O.R. Moheimani, Minimizing the effect of out of bandwidth modes in truncated structure models, J. Dyn. Syst. Meas. Control. 122 (1) (1998) 237–239.

[21] C. Harkort, J. Deutscher, Finite-dimensional observer-based control of linear distributed parameter systems using cascaded output observers, Internat. J. Control 84 (1) (2011) 107–122.

[22] I. Lasiecka, R. Triggiani, Stabilization and structural assignment of Dirichlet boundary feedback parabolic equations, SIAM J. Control Optim. 21 (5) (1983) 766–803.

[23] R.F. Curtain, Finite dimensional compensators for parabolic distributed systems with unbounded control and observation, SIAM J. Control Optim. 22 (2) (1984) 255–276.

[24] I. Karafyllis, M. Krstic, ISS with respect to boundary disturbances for 1-D Parabolic PDEs, IEEE Trans. Autom. Control 61 (12) (2016) 1–23.

[25] I. Karafyllis, M. Krstic, Input-to-State Stability for PDEs, Springer International Publishing, Cham, 2019.

[26] R. Katz, E. Fridman, Constructive method for finite-dimensional observer-based control of 1-D parabolic PDEs, Automatica 122 (2020) 109285.

[27] I. Karafyllis, Lyapunov-based boundary feedback design for parabolic PDEs, Internat. J. Control 94 (5) (2021) 1247–1260.

[28] A. Selivanov, E. Fridman, Boundary observers for a reaction–diffusion system under time-delayed and sampled-data measurements, IEEE Trans. Autom. Control 64 (8) (2019) 3385–3390.

[29] H. Lhachemi, C. Prieur, Predictor-based output feedback stabilization of an input delayed parabolic PDE with boundary measurement, Automatica 137 (2022) 110115.

[30] R. Katz, E. Fridman, Delayed finite-dimensional observer-based control of 1D parabolic PDEs via reduced-order LMIs, Automatica 142 (2022).

[31] R. Katz, E. Fridman, Global stabilization of a 1D semilinear heat equation via modal decomposition and direct Lyapunov approach, Automatica 149 (2023) 110809.

[32] A. Selivanov, P. Wang, E. Fridman, Guaranteed cost boundary control of the semilinear heat equation, IEEE Control. Syst. Lett. 8 (2024) 898–903.

[33] R. Katz, E. Fridman, Finite-dimensional boundary control of the linear Kuramoto-Sivashinsky equation under point measurement with guaranteed L2-gain, IEEE Trans. Autom. Control 67 (10) (2022) 5570–5577.

[34] A. Selivanov, E. Fridman, Finite-dimensional boundary control of a wave equation with viscous friction and boundary measurements, IEEE Trans. Autom. Control (2023) 1–8.

[35] A. Selivanov, E. Fridman, Disturbance attenuation in the Euler–Bernoulli beam with viscous and Kelvin–Voigt Damping via piezoelectric actuators, in: 62nd IEEE Conference on Decision and Control, 2023, pp. 1961–1966.

[36] J. Bontsema, R.F. Curtain, J.M. Schumacher, Robust control of flexible structures A case study, Automatica 24 (2) (1988) 177–186.

[37] K. Lenz, H. Özbay, Analysis and robust control techniques for an ideal flexible beam, in: C.T. Leondes (Ed.), Control and Dynamic Systems, vol. 57, Academic Press, 1993, pp. 369–421.

[38] D. Halim, S.O. Moheimani, Spatial resonant control of flexible structures - application to a piezoelectric laminate beam, IEEE Trans. Control Syst. Technol. 9 (1) (2001) 37–53.

[39] M. Tucsnak, Regularity and exact controllability for a beam with piezoelectric actuator, SIAM J. Control Optim. 34 (3) (1996) 922–930.

[40] E. Crépeau, C. Prieur, Control of a clamped-free beam by a piezoelectric actuator, ESAIM - Control. Optim. Calc. Var. 12 (3) (2006) 545–563.

[41] Y. Bai, C. Prieur, Z. Wang, Exact controllability for a Rayleigh beam with piezoelectric actuator, Systems Control Lett. 186 (2024) 105759.

[42] D. Halim, S. Moheimani, Experimental implementation of spatial H-infinity control on a piezoelectric-laminate beam, IEEE/ASME Trans. Mechatronics 7 (3) (2002) 346–356.

[43] A. Belyaev, A. Fedotov, H. Irschik, M. Nader, V. Polyanskiy, N. Smirnova, Experimental study of local and modal approaches to active vibration control of elastic systems, Struct. Control. Heal. Monit. 25 (2) (2018).

[44] D.L. Russell, On mathematical models for the elastic beam with frequency-proportional damping, in: Control and Estimation in Distributed Parameter Systems, Society for Industrial and Applied Mathematics, 1992, pp. 125–169.

[45] L. Herrmann, Vibration of the Euler–Bernoulli beam with allowance for dampings, in: World Congress on Engineering, 2008, pp. 901–904.

[46] E.F. Crawley, J. De Luis, Use of piezoelectric actuators as elements of intelligent structures, AIAA J. 25 (10) (1987) 1373–1385.

[47] C.R. Fuller, S.J. Elliott, P.A. Nelson, Active Control of Vibration, Elsevier, 1996.

[48] G. Chen, D.L. Russell, A mathematical model for linear elastic systems with structural damping, Quart. Appl. Math. 39 (4) (1982) 433–454.

[49] A. Pazy, Semigroups of Linear Operators and Applications to Partial Differential Equations, Springer, New York, 1983, p. 44.

[50] M. Tucsnak, G. Weiss, Observation and Control for Operator Semigroups, Birkhäuser Basel, 2009.

[51] S. Timoshenko, Strength of Materials. Part 1, Van Nostrand, 1955.

[52] H.T. Banks, D.J. Inman, On damping mechanisms in beams, J. Appl. Mech. 58 (3) (1991) 716–723.